Water Research 267 (2024) 122412

Contents lists available at ScienceDirect

Water Research

journal homepage: www.elsevier.com/locate/watres

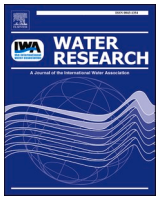

Tracing pesticide dynamics: High resolution offers new insights to karst groundwater quality

Johannes Schorr [a,b], Franziska Jud [a], Daniele la Cecilia [a,c], Birgit Beck [a], Philipp Longree [a], Heinz Singer [a], Juliane Hollender [a,b,*]

[a] Eawag: Swiss Federal Institute of Aquatic Science and Technology, Überlandstrasse 133, 8600 Dübendorf, Switzerland
[b] Institute of Biogeochemistry and Pollutant Dynamics, Universitätstrasse 16, ETH Zürich, 8092 Zürich, Switzerland
[c] Department of Civil, Environmental and Architectural Engineering, University of Padova, Via Marzolo 9, 35131 Padova, PD, Italy

ARTICLE INFO

Keywords:
In-situ monitoring
Liquid chromatography high-resolution mass spectrometry
Karst groundwater
Pesticides
Pesticide transformation products
Drinking water

ABSTRACT

Generally, karst aquifers and springs are highly susceptible to contamination due to the high permeability and, therefore, groundwater flow velocities. The often thin soil cover, accompanied by dolines, can lead to fast infiltration of precipitation water loaded with mobilized contaminants such as pesticides and their transformation products. To date, continuous, temporally highly resolved in-situ monitoring to decipher concentration dynamics for a broad range of pesticides is missing. Therefore, a transportable HPLC-HRMS/MS system (MS^2field) was positioned at two karst study sites in the Swiss Jura. Water samples were collected and analyzed for pesticides and their transformation products in-situ every 20 min for 6 weeks in 2021 and 8 weeks in 2022. During the spraying season in 2021, six rain events at site 1 and three at site 2 in 2022 were captured. Concurrently, the water quality parameters electrical conductivity, pH, nitrate, turbidity, and water level, were monitored continuously at high temporal resolution. Further, bacterial cell counts were monitored via online flow cytometry.

In 2021, several pesticides and pesticide transformation products were detected in peak concentrations after rain events, of which metamitron showed the highest concentration of up to 1000 ng/L. In one rain event, the Swiss federal and EU drinking water limit of 100 ng/L was exceeded for up to 38 h. Compared with highly frequent MS^2field samples collected every 20 min, 42-hours composite samples severely underestimated peak concentrations for all compounds, especially for labile ones. Therefore, it was demonstrated that exceedences of the regulatory limit would have been missed if just composite sampling would have been conducted. Peak concentrations of pesticides coincided with peaks in nitrate concentration and bacterial cell counts following rain events. The correlation analysis showed strong correlations between the three analyzed contaminants (pesticides, nitrate and bacteria), and the proxy parameters electrical conductivity, and pH. The investigation of a second spring revealed similar dynamics indicating that these can be expected in other karst aquifers as well.

1. Introduction

Estimates suggest that between 10 % (Parise et al., 2018) and 25 % (Ford and Williams, 2007) of the global population rely on karst groundwater as their primary source of drinking water. Since these numbers are complicated to assess, the percentage of people living in karst areas reported by Goldscheider et al. (2020) might provide a better estimate (16.5 % in 2015). In Switzerland, about 18 % of the drinking water is produced or taken without much pretreatment from karst aquifers (FOEN, 2019). Compared to sedimentary aquifers with a comparably low hydraulic conductivity, large cavities can develop through persistent dissolution of the rock matrix along fissures and cracks in carbonate rock. Eventually, this can lead to preferential flow paths, high hydraulic conductivities, and, therefore, high groundwater

Abbreviations: EC, electric conductivity; ESI, electrospray ionization; GUS, groundwater ubiquity score; HPLC, high performance liquid chromatography; HRMS/MS, high resolution tandem mass spectrometry; ILIS, isotopically labelled internal standard; LOQ, limit of quantification; RPLC, reversed phase liquid chromatography; STD, reference standard; TP, transformation product.

* Corresponding author.
E-mail address: juliane.hollender@eawag.ch (J. Hollender).

https://doi.org/10.1016/j.watres.2024.122412
Received 27 March 2024; Received in revised form 30 August 2024; Accepted 6 September 2024
Available online 14 September 2024

velocities (Medici and West, 2021; Worthington and Ford, 2011). The rate of dissolution, hence the formation rate of cavities or preferential flow paths, depends highly on the local conditions, i.e. hydraulic gradient, mineral composition, topography, soil cover, vegetation, climate, etc. and is thus subject to change over geologic timescales (Bakalowicz, 2005; Ford and Williams, 2007). As a result, karstification varies strongly between locations, leading to significant differences in hydrogeologic properties, e.g. hydraulic conductivity (Medici and West, 2021).

Due to large (vertical) cavities enabling preferential flow, infiltrating meteoric water can bypass zones with lower permeability along with their enhanced filter capacity (Ravbar and Goldscheider, 2007). Moreover, karst aquifers often feature a thin or absent overlaying soil cover (typically "filtering" contaminants by adsorption and degradation) and, therefore, have a high intrinsic vulnerability towards contamination (Coxon, 2011; Epting et al., 2018). These properties enable the fast transport of mobile contaminants like chemicals (Hillebrand et al., 2012; Reh et al., 2014; Reh et al., 2016; Schiperski et al., 2015) or microbial cells (Besmer et al., 2017; Butscher et al., 2011; Kaiser et al., 2022; Pronk et al., 2007) which can result in peak concentrations during or after rain events. Increased cell numbers during rain events can be associated with faecal indicator organisms such as E. coli or Enterococcus (Besmer et al., 2017), making it an essential parameter for monitoring raw water quality used for drinking water production from karst springs. Moreover, during rain events, chemicals present at the catchment surface or in the soil or rock matrix can be mobilized, infiltrated and transported to karst springs. Despite the high permeability of karstified aquifers, some contaminants can still accumulate in the soil and rock matrix with slower flow, which can result in their continuous release over long periods (Kiefer et al., 2020; Morasch, 2013; Padilla and Vesper, 2018). Depending on land-use in the catchment, these compounds include wastewater contaminants (Zemann et al., 2015; Zirlewagen et al., 2016), industrial emissions (Metcalfe et al., 2011; Reberski et al., 2022), legacy compounds from contaminated sites (Padilla and Vesper, 2018; Vesper et al., 2001), tire wear particle leachates (Tian et al., 2021) and pesticides and their transformation products (TP) (Reh et al., 2013; Schorr et al., 2023). Thereof, pesticides are an exceptionally critical group of compounds due to their deliberate introduction into the environment and their intentional toxicity.

Besides the aquifer properties, compound physicochemical properties like adsorption affinity and stability can determine the probability of a compound breaking through and resulting in peak concentrations at a karst spring during a rain event. Mobility, or leachability of a compound, can be assessed jointly, relating the half-life (DT_{50}) in soil with the adsorption to soil, given as the compound's log K_{OC}, to obtain the groundwater ubiquity score (GUS (Gustafson, 1989)). "Potential leachers" are those for which the GUS value is higher than 2.8, while "nonleachers" would have a GUS lower than 1.8, leaving a transition zone of moderate leachability between these two cut-off values. However, as Gustafson (1989) points out, the concept of leachability, as defined therein, is only applicable where no direct connection between surface and saturated zones exists. This is not the case in karst, as preferential flow paths are known to exist. Hence, the leachability of pesticides in karst is not trivial to predict (Schaffer and Licha, 2015). The insufficient predictability of leachability of pesticides in karst demonstrates the unchanged need for appropriate sampling strategies and monitoring approaches.

Several studies have investigated the occurrence of pesticides and urban pollutants in karst aquifers, however, with varying objectives and, therefore, also differing sampling strategies (Schiperski et al., 2015; Selak et al., 2023). While occasional grab samples or 2-week composite samples may suffice to monitor background concentrations, dynamic changes can lead to unnoticed contamination using those strategies (Hillebrand et al., 2014; Schiperski et al., 2015; Selak et al., 2023). Doummar et al. (2014) acknowledged that concentrations of substances in karst groundwater can change rapidly in the order of hours. However, concentration dynamics of organic substances, particularly pesticides, in karst springs following precipitation events have not yet been examined for numerous compounds nor at temporal resolutions finer than 3–6 h (Doummar et al., 2014; Hillebrand et al., 2014; Morasch, 2013; Reh et al., 2013; Zirlewagen et al., 2016). The small number of pesticides investigated therein allows only a limited transferability to the wide range of compounds being used in agriculture. Morasch (2013) found atrazine and chloridazon at concentrations reaching the low µg/L range. However, the biweekly sampling frequency was low compared to the dynamics potentially taking place. The choice of a fitting sampling strategy determines what type of concentration dynamics can be observed, and sampling at a high temporal resolution for karst aquifers was deemed crucial before (Epting et al., 2018; Reberski et al., 2022; Reh et al., 2014). In contrast, the current Swiss national groundwater monitoring program NAQUA, like many national monitoring programs, involves a sampling frequency of only up to 2 grab samples per year, which does not allow for monitoring short-term concentration dynamics (FOEN, 2019).

Therefore, this study aimed to examine the temporal dynamics of the concentrations of different pesticides and pesticide TPs with varying properties in two agriculturally impacted Swiss karst springs following precipitation events. The expected fast concentration changes were monitored by analyzing karst groundwater in-situ at unprecedented high temporal resolution provided by the transportable high-performance liquid chromatography (HPLC) – electrospray ionization (ESI) – high-resolution mass spectrometry (HRMS/MS) platform MS^2field (Stravs et al., 2021). Large volume direct injection of the samples allowed for sufficiently low quantification limits (low ng/L range), while the HRMS/MS detection allowed screening for many analytes simultaneously. Besides the MS^2field, 42 h-composite samples were obtained to study the effects of lower sampling frequencies on detected pesticide concentrations. In addition to pesticides and their TPs, the total cell count and physicochemical parameters such as turbidity and electrical conductivity (EC) were monitored in a high temporal resolution to assess their correlations with pesticide concentration dynamics and, consequently, their suitability for predicting pesticide concentration changes.

2. Materials and methods

2.1. Study sites

Two karst springs in the Swiss Jura, thereafter referred to as sites 1 and 2, were selected for comparative pesticide monitoring. Both catchments were dominated by agriculture (40 % and 60 %, Table 1.1 and 1.2, resp., SI-A). However, this study will focus on results from site 1 from 2021 since the pronounced dry period during the monitoring of site 2 in 2022 led to only very small rain events. Yet, a brief comparison of the two sites is presented in Section 3.6.

In 2021, site 1 was investigated during ca. 6 weeks from April to June with the MS^2field and from April to October using 42 h-composite samples. Land use in the catchment of site 1 included: (winter-) barley, (sugar-) beet, (green-, silage-) maize, meadows, potato, (winter-) rapeseed to produce oil and (feed-, winter-) wheat. On a voluntary basis, farmers kindly provided crop and application data of pesticides for the years 2020, 2021 and 2022. The catchment area comprised 7.7 km^2, and the sampled spring had an average discharge of ~2000 L/min (min.: 600–1200 L/min; max.: >20,000 L/min). Every night, spring water is abstracted and pumped into a reservoir (Fig. 4). The average monthly precipitation for this region during the last 30 years was quite steady throughout the year and ranges between 80 mm and 110 mm each month. However, during the field campaign 2021, exceptionally high precipitation was observed in January, May, June and July (Figure 1.1, SI-A). On the contrary, February through April, and August through November received much less precipitation (ca. 50 mm) than on average.

The phreatic aquifer is situated in karstified limestone mainly of the tabular, upper Jurassic. The regional aquiclude consists of Oxford marls and no surface water bodies are present. The mean aquifer thickness (from aquiclude to the land surface) amounts to ~140 m while the saturated zone varies from 60 to 100 m. Past tracer tests (data not shown) revealed groundwater flow velocities between 20 and 70 m/h in medium to highly conductive hydraulic conductivities (FOEN, 2023). Soils in the catchment are mostly less than 1 m, sometimes up to 1.5 m thick and consist of silty loamy brown earths or occasionally pseudogleys (NABODAT, 2024). The variability in soil thickness is high throughout the catchment, with fast draining, thin soils alternating with slower draining, thicker soils.

2.2. Data acquisition and sampling

From mid April to the end of October 2021, the electrical conductivity, nitrate, pH, precipitation, turbidity and the water level were continuously monitored in-situ, at a high temporal resolution (for details see SI-A 1). In the same period, 42 h-composite samples were taken by sampling every 15 min for 42 h, yielding 4 samples per week of which ~80 mL each were collected in clear glass bottles (SIMAX, 100 mL, Huberlab. AG, Switzerland) from the chilled sampler (5 °C, TP5 C, MAXX GmbH, Germany) and stored frozen and dark until analysis.

From 28.04.2021 to 10.06.2021, the on-site, in-situ monitoring was performed with the MS^{2}field, a mobile mass spectrometer, presented in detail elsewhere (Stravs et al., 2021). A continuous water flow from the karst spring through the trailer was established, from which one filtered (3–5 μm mesh size) sample per 20 min was abstracted and injected to the HPLC-HRMS/MS system (see Section 2.4). In total, this resulted in 2493 samples over the 6 weeks monitoring period. In addition to the online monitoring of micro-pollutant concentrations, the total cell count (TCC) was monitored by online flow cytometry. An Accuri C6 flow cytometer (BD Accuri, San Jose CA, USA) was connected to the water bypass via a custom-made 10-port-valve module such that every 15 min, a sample was obtained and analyzed automatically. Following the protocol in Besmer et al. (2014), the sample was spiked with SYBR^{TM} Green I nucleic acid gel stain (Invitrogen^{TM}, Thermo Fisher Scientific, U.S.; diluted 1:10, 000 in sterile TRIS buffer at 10 mM and pH 8.0), incubated for 10 min at 37 °C, and subsequently, 100 μL were injected into the analyzer. Detection was performed by using a blue laser emitting at 488 nm and by collecting fluorescence intensity at FL1 = 533±30 nm and FL3 > 670 nm (Prest et al., 2013).

2.3. Chemicals and standards

The list of target compounds, screened for their occurrence in karst groundwater included 289 chemicals, mainly pesticides and their TPs with some additional wastewater markers (SI-B 1). The chemicals were chosen based on prior findings in the Swiss national groundwater monitoring program NAQUA, analyzability with HPLC-ESI-HRMS/MS and availability of reference standards (STD). Reference standards and 124 isotopically labelled internal standards (ILIS, SI-B) were combined into STD and ILIS mixtures, respectively and stored at −20 °C until usage. STD and ILIS mixtures used in the MS^{2}field were prepared in evian® mineral water to reduce adsorption to the glass vials in which they were stored and hence, improving recoveries and reproducibility. Ultrapure water used in this study was taken from an ultrapure water system (Arium® Pro, Sartorius, Germany) and methanol was of LC/MS grade (Optima^{TM}, Fisher Chemical, U.S.). Further, the sampling tubing in the MS^{2}field was cleaned after each sampling with a 80:20 v:v mixture of ultrapure water:evian®. This was followed by a cleaning step with ethanol (Ethanol absolut A15+5 % IPA, Reuss Chemie, Switzerland).

2.4. HPLC-HRMS/MS analyses

MS^{2}field samples (250 μL) were automatically taken from the continuously flowing water bypass with a dilutor syringe connected to a 6-port valve. From two ports, ILIS and STD mix solutions were added to the samples, such that a final ILIS concentration of 200 ng/L resulted in the samples. Every 10th sample was spiked with STD to reach a concentration of 200 ng/L either in karst groundwater, or in 80:20 (v:v) ultrapure H_2O:evian®, thereafter called spikes and quality control samples, respectively. This procedure allowed for a continuous quality assurance and therefore ensured robust instrument performance over time. Before each new sequence (ca. once per week), a calibration series was prepared automatically and injected to the HPLC-ESI-HRMS/MS system at 2, 5, 10, 20, 50, 100, 200, 400, 1000, 2000, 5000 ng/L in 80:20 (V:V) ultrapure H_2O:evian®. The automatically prepared samples were injected to the HPLC via large volume direct injection (250 μL) and eluted at a flow rate of 300 μL/min. To remove small particulates and to aid separation, the sample was first passed through a self-packed pre-column (stainless steel, 2.1×20 mm, BGB Analytik AG, Switzerland) containing Atlantis® T3 material (10 μm, Waters, Ireland). Then, analytes were separated on a reverse phase analytical column (Atlantis® T3 5 μm, 3.0×50 mm, Waters, Ireland). Note the shorter length of this column compared to laboratory based analysis to allow one measurement every 20 min. Similar to laboratory analysis, elution was achieved by an ultrapure water, methanol gradient at 300 μL/min (SI-A). Since in the MS^{2}field, no sample can be measured twice, the instrument (Q Exactive^{TM} HF with ESI source, Thermo Fisher Scientific, U.S.) was run in switching mode (−3.0, 4.0 kV). The first 4 min of the eluate was sent to waste to protect the mass spectrometer. Details on the method are provided in Table 1.4 (SI-A).

The 42 h-composite samples were analyzed in the laboratory using the same analytical column although in a longer version (150 mm) and also an Orbitrap instrument (Q Exactive^{TM} Plus, Thermo Fisher Scientific, U.S.). Here, samples were however measured separately in positive and negative mode (for details on lab analysis see SI-A 2).

2.5. Quantification and method validation

Data evaluation for lab samples and MS^{2}field samples was performed using TraceFinder^{TM} 5.1 (Thermo Fisher Scientific, U.S.). Due to the high number of samples from the MS^{2}field analysis, samples acquired during rain events were first screened qualitatively for the above mentioned 289 compounds and only the detected compounds were then quantified in all samples. For the lab method, recovery samples were used to calculate matrix factors and relative recoveries (Eq's. 2.1 to 2.7, SI-A). For the MS^{2}field, these parameters were calculated based on the average concentration in two samples measured directly before and after the spiked sample. The accuracies and the precisions of the two methods were calculated for each analyte as the average relative recovery and the relative standard deviation of the relative recovery, respectively. The method limits of quantification (LOQ) were calculated as the ultrapure water LOQ corrected by the matrix factor, respectively. As the internal standard calibration method was used for quantification, concentrations of compounds that did not have a matching ILIS were corrected by their respective relative recovery.

The LOQs in groundwater ranged between 1.9 ng/L and 50 ng/L (median 11 ng/L) with the MS^{2}field method, and between 1.8 ng/L and 22 ng/L with the lab-based method (median 5.4 ng/L, SI-B 2). The slightly higher median LOQ in the MS^{2}field was attributed to the shorter analytical column in the MS^{2}field and most likely stronger matrix interference due to less chromatographic separation. The accuracy and the precision were excellent for both methods with average values of 98 % and 8 % in the MS^{2}field which are comparable to values reported elsewhere for this instrumentation (la Cecilia et al., 2021; Stravs et al., 2021), and 96 % and 10 % in the lab method. All detected substances were identified unequivocally with their reference standard, in most cases a matching internal standard and in all cases with their MS2-spectrum (SANTE/12682/2019, 2019).

2.6. Statistical analysis

For statistical analysis, i.e. Spearman correlation, data gaps in the time series of all monitored parameters were filled by linear interpolation. MS^{2}field values below the LOQ were replaced with values drawn randomly from a normal distribution with half the respective LOQ as the mean and a 10 % standard deviation around that mean. In order to temporally align the time series of different parameters, they were resampled at a 20 min resolution using linear interpolation.

The non-parametric spearman's correlation (ρ) was calculated, which is more robust in the presence of outliers and does not require a linear relationship between the parameters (Dormann, 2013). Only significant correlations (p-value < 0.05) were retained for analysis. Moreover, since pesticide peak heights were different in every event, they were treated separately and correlation coefficients for each event were calculated.

Before spearman's ρ was calculated, the ranked time series were checked for their monotonic relationship. For some combinations, e.g. pH vs. nitrate the data pairs scattered monotonically, in this case even linearly (SI-C). For others, e.g. metamitron vs. EC, a hysteresis effect could be observed which was obviously not removed via the rank transformation. This effect is due to the asynchronous nature of the detected signals and was observed before in karstic environments (Schiperski et al., 2015; Stroj et al., 2020) but still hints towards a strong correlation between the variables.

3. Results and discussion

3.1. Pesticide applications vs. detections in the karst spring

In 2021, at least 70 pesticides (65 synthetic organic chemicals) were applied in the catchment of site 1, totaling at least 215 kg. For comparison, ca. 300 kg of pesticides were applied each year in 2020 and 2022. In 2021, about 105 kg were applied before or during the MS^{2}field sampling period (Table 2.5, SI-A). The 70 pesticides included 34 herbicides, 15 fungicides, 13 insecticides, 1 molluscicide, 5 plant growth regulators and 2 additives (SI-B). Land use in the catchment included 15 types in 2021. The crops that received the largest share of pesticides were corn (58.2 kg), barley (44.4 kg), wheat (39.4 kg), rapeseed (26.2 kg), winter crops (24.4 kg) and beet (19.9 kg), making up 97 % of the total applied mass in 2021.

Forty-five of the 70 applied compounds were analyzed with either of the two reversed phase liquid chromatography (RPLC)-based sampling strategies presented here or with the ion chromatography (IC)-based method for anionic compounds presented in Schorr et al. (2023), where the same 42 h composite samples were screened for very polar and anionic compounds (e.g. chlorothalonil TP SYN548008). Both, the RPLC methods presented here and the IC method presented by Schorr et al. (2023), specifically targeted compounds in the polar range since these were expected to leach into the groundwater. Of the 45 analyzed compounds, 11 were detected (Fig. 1). Three compounds in the low leachability range (bromoxynil: 1.7, mesotrione: 1.5, prochloraz: 1.6), 5 in the moderate leachability range (chlortoluron: 2.0, dimethenamid: 2.4, epoxiconazole: 2.1, metamitron: 2.2, tebuconazole: 1.9) and 3 in the high leachability range (ethofumesat: 3.0, foramsulfuron: 3.0, mesosulfuron-methyl: 3.9) were detected. The median GUS of 1.46 of the 34 non-detected compounds was in the low leachability range (GUS = 0–1.8), while the median GUS of 2.09 of the 11 detected compounds was in the moderate leachability range (GUS = 1.8–2.8). This indicates the applicability of the GUS to predict potential breakthrough compounds in karst.

The non-detection of compounds in the low leachability range applied in high amounts (e.g. ethephon, glyphosate, pendimethalin, or prothioconazole) was most likely due to adsorption and degradation in the soil. The 25 non-analyzed compounds included very apolar compounds like pyrethroids (high log P values; e.g. lambda-cyhalothrine, applied amount: 0.1 kg), which were not expected to leach and often not amenable to the analytical method used here (pyrethroids). Their median GUS of 0.3 hints towards immobility. Moreover, the total amount of non-analyzed synthetic organic pesticides excluding copper and rapeseed oil was relatively low (ca. 27 kg, SI-B 3).

Compounds such as clomazone, dicamba, napropamide, and terbuthylazine, which were applied in comparable quantities and exhibited a GUS similar to metamitron within the moderate leachability range, were not detected. Their non-detection could be due to (a) application outside of precipitation-intense periods (e.g. clomazone, application in August),

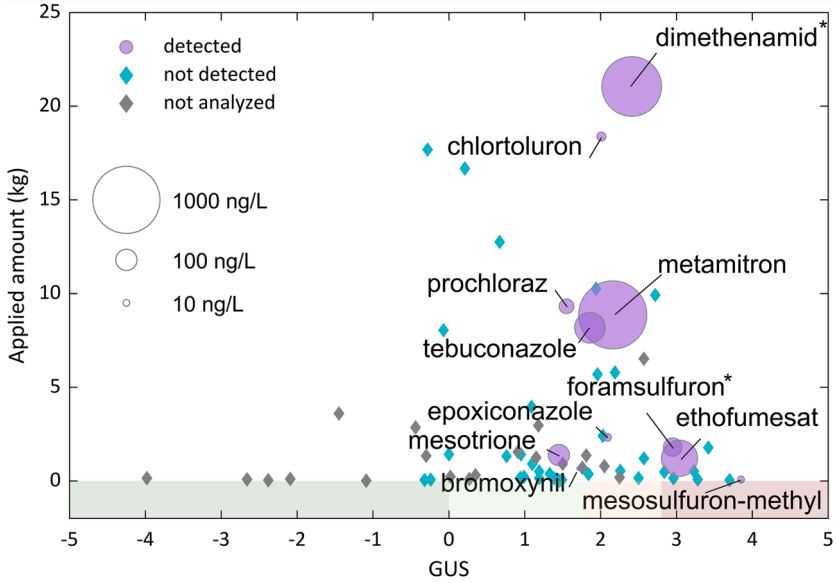

Fig. 1. This figure shows the applied amount vs. the GUS value of all compounds that were applied in 2021 in catchment of spring 1. They are categorized into compounds that were detected, not detected and not analyzed. The size of the circles relates to the maximum concentration detected. Here, the maximum conc. of dimethenamid and foramsulfuron (*) were detected outside the MS^{2}field monitoring campaign in 42 h-composite samples. The colored bar in the lower part of the figure classifies the leachability as follows: Dark-green: extremely low, light-green: low, light-red: moderate, dark-red: high (Gustafson, 1989). For details on non-annotated compounds refer to SI-B 3.

(b) dilution in 42 h-composite samples during rain event while having been applied outside of the MS^{2}field monitoring period, (c) instability of the compound in stored samples or (d) adsorption to sampling container or other sample preparation equipment. The non-detection of dicamba, for example, was remarkable on the one hand due to its high GUS of 1.94, and on the other hand due to its application during the rain-intense period in May and June 2021 (SI-B) with a total applied amount of 10 kg. Possibly, the fast photolytic degradation within days after application (Gruber et al., 2021) and the relatively high LOQ of 50 ng/L in the MS^{2}field and 20 ng/L in the lab method lead to the non-detection. Additionally, dilution in and storage of the composite samples possibly decreased the analyte's concentration.

3.2. Detections – MS2field vs. 42 h-composite samples

Of the 289 screened chemicals, 15 were found and quantified in 2493 samples from the 6-week MS^{2}field monitoring period (11 parents, 3 TPs, genistein). 29 compounds (19 parents, 10 TPs) were found and quantified in 86 42 h-composite samples from April to October 2021 (Table 1). Hence, 14 compounds were found in the 42 h-composite samples but not in the MS^{2}field samples. Most of these additional detections were made outside the MS^{2}field monitoring period (column 5, Table 1) since some pesticides were applied only after that period (ca. 50 % of the total applied mass in 2021). For a few analytes, their detection in the 42 h-composite samples and not in the MS^{2}field was due to the longer analytical column in the lab method, leading to better peak shapes, and therefore, lower LOQs (i.e. for dimethachlor CGA 369873 or chlorothalonil TPs).

Contrastingly, genistein, mesotrione (GUS = 1.45) and prochloraz (GUS = 1.55) were found only with the MS^{2}field method. Their non-detection in 42 h-composite samples, was likely due to dilution in the composite samples (calculated mean for genistein: 29 ng/L vs. LOQ = 40 ng/L). Other reasons possibly include degradation ($DT50_{soil}$: genistein: unknown, mesotrione = 5–20 d, prochloraz = 70–120 d, (Lewis et al., 2016)) and adsorption (log D_{OW}: genistein = 2.5, mesotrione = −1 and prochloraz = 3.6 (pH 7, ChemAxon, 2023, respectively) during sample storage and preparation.

In the period when both monitoring strategies were operating, 11 compounds were detected by both sampling methods, 4 (genistein, mesotrione, nicosulfuron and prochloraz) were only detected by the MS^{2}field, and 3 (dimethachlor CGA 369873 and chlorothalonil TPs) were only detected in the 42 h-composite samples. Hence, not only did the MS^{2}field provide more substance detections, showing that the dilution effect outweighed the higher LOQs, but it also measured the realistic maximum concentrations. The dilution effect, leading to generally lower concentrations in composite samples, was observed for several compounds (Table 1; more details for metamitron in Section 3.3 and Fig. 2). For compounds detected with both methods, the accurateness of the concentrations measured with the MS^{2}filed were confirmed. For example, in event five, the calculated average concentrations of metamitron and metamitron-desamino for 42 h were 240 ng/L and 83 ng/L, which in the corresponding 42 h-composite sample, were 240 ng/L and 110 ng/L, respectively.

Based on the results acquired at high temporal resolution, it may be concluded that the sporadic detections over 100 ng/L measured in previous monitoring campaigns (e.g., for chlortoluron, ethofumesat or metamitron analyzed from 2007 to 2014 in the Swiss national groundwater monitoring program NAQUA) were likely caused by the low

Table 1
Detected compounds at site 1, in 2021. In column 4, the maximum concentration measured with either methods during the MS^{2}field monitoring period is reported and in the 5th column, the maximum concentration measured outside the MS^{2}field period is reported. GUS values from Lewis et al. (2016). Number of samples included MS^{2}field / 42 h-composite: 2493 / 86. Abbreviations: f.: fungicide, h.: herbicide, iso.: isoflavone, n.q.: not quantified, n.d. not detected. Pesticides detected in concentrations above 100 ng/L are bold. For toxicologically non-relevant TPs the 100 ng/L does not apply. (a) Exclusively found in composite samples, (b) Parent substance applied, (c) Application prohibited in karst.

Compound	Type	GUS	Max conc.: MS^{2}field / 42 h (ng/L)	Max. conc. 42 h outside MS^{2}field period (ng/L)	Number of samples > LOQ	Applied
Atrazine	h.	2.6	17 / 14	14	1333 / 86	–
Atrazine-desethyl	TP	–	38 / 38	38	2112 / 86	–
Atrazine-desisopropyl	TP	–	n.d. / n.d.	5	n.d. / 4	–
Bromoxynil	h.	1.7	n.d. / n.d.	3 [(a)]	n.d. / 2	X
Chloridazon-methyl-desphenyl	TP	–	**140** / **110**	**140**	2293 / 86	–
Chlorothalonil R417888	TP	–	n.q. / 28 [a)]	36 [(a)]	n.q. / 65	–
Chlorothalonil R471811	TP	–	n.q. / **340**	**410** [(a)]	n.q. / 86	–
Chlortoluron	h.	2.0	18 / 6	3	19 / 7	X
Dimethachlor CGA369873	TP	–	n.d. / 15	18 [(a)]	n.d. / 32	X [(b)]
Dimethenamid	h.	2.4	38 / 17	**790**	67 / 29	X
Epoxiconazole	f.	2.1	14 / 10	8	61 / 7	X
Ethofumesate	h.	3.0	**290** / 62	n.d.	44 / 1	X
Fluxapyroxad	f.	2.6	n.d. / n.d.	9 [(a)]	0 / 6	X
Foramsulfuron	h.	3.0	n.d. / n.d.	76 [(a)]	0 / 10	X
Genistein	iso.	–	**170** / n.d.	n.d.	28 / n.d.	–
Haloxyfop	h.	2.4	n.d. / n.d.	10 [(a)]	n.d. / 1	X
Mesosulfuron-methyl	h.	3.9	n.d. / n.d.	11 [(a)]	n.d. / 1	X
Mesotrione	h.	1.5	**100** / n.d.	n.d.	19 / n.d.	X
Metalaxyl CGA62826	TP	–	n.d. / m.d.	5 [(a)]	n.d. / 1	–
Metamitron	h.	2.2	**1030** / **240**	**300**	757 / 32	X
Metamitron-desamino	TP	–	**350** / **110**	41	237 / 47	X [(b)]
Metazachlor ESA	TP	–	n.d. / n.d.	37 [(a)]	n.d. / 9	–
Metolachlor	h.	2.4	**340** / 82	32	470 / 6	–
Napropamid	h.	2.0	n.d. / n.d.	8 [(a)]	n.d. / 1	X
Nicosulfuron	h.	3.4	25 / n.d.	12 [(a)]	1 / 1	X
Prochloraz	f.	1.6	48 / n.d.	n.d.	1 / n.d.	X
Prometon / Terbumeton	h.	6.3 / 3.8	n.d. / n.d.	6 [(a)]	n.d. / 1	–
Propamocarb	f.	–	n.d. / n.d.	11 [(a)]	n.d. / 2	–
Propazine / Terbuthylazine	h.	3.9 / 2.2	n.d. / n.d.	12 [(a)]	n.d. / 6	X [(c)]
Tebuconazole	f.	1.9	**210** / 83	36	1160 / 52	X
Terbuthylazine CSCD648241	TP	–	n.d. / n.d.	11 [(a)]	n.d. / 1	X [(b)]
Thiencarbazone-methyl	h.	2.5	n.d. / n.d.	28 [(a)]	n.d. / 2	X

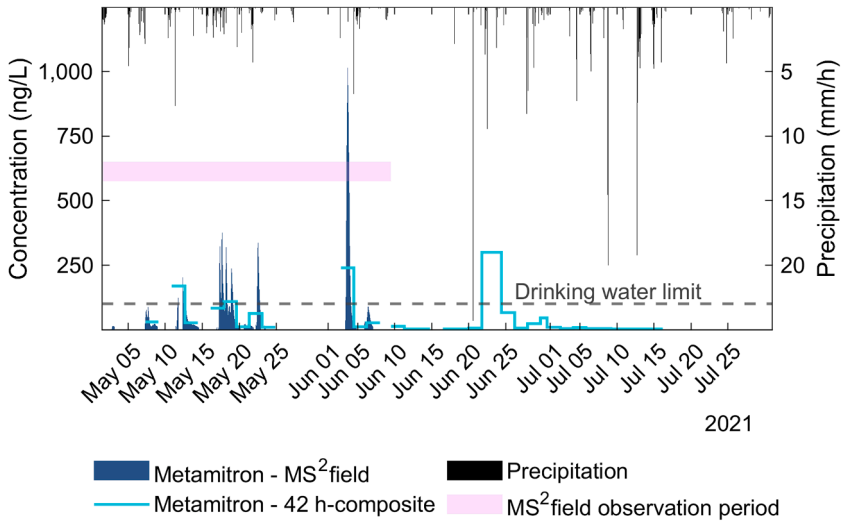

Fig. 2. Measured concentrations in MS^{2}field samples (dark blue) and 42 h-composite samples (light blue). The MS2field measurements were conducted from the end of April until the beginning of June while the 42 h-composite samples were obtained from mid April until the end of October 2021.

sampling frequency and the sampling timing vs. the timing of application and rain.

3.3. Dynamics of pesticides and transformation products

3.3.1. Legacy compounds

Transformation products of phased-out pesticides that leach continuously into the groundwater at site 1 included atrazine-desethyl, atrazine-desisopropyl, chloridazon-methyl-desphenyl (Fig. 3), 4 chlorothalonil TPs, of which 2 were found only using ion-chromatography (Schorr et al., 2023) and also the parent compound atrazine, although banned in Switzerland since 2012 (FOEN, 2023). The continuous detection of atrazine and its TPs was expected (la Cecilia and Maggi, 2017) as these substances are ubiquitously present in agriculturally used areas worldwide and in Switzerland (Maggi et al., 2019). The less frequent detection of atrazine-desisopropyl is in agreement with literature reports (Baran et al., 2008; Kolpin et al., 2004; Reh et al., 2014), and here the sporadic detections around the LOQ hint towards a continuous release along with atrazine and atrazine-desethyl.

The continuously leaching, non-relevant TP chloridazon-methyl-desphenyl is widely detectable in considerable concentrations in groundwater in the Swiss NAQUA monitoring (>100 ng/L at 14 % of the monitoring wells (FOEN, 2020)). The 42 h-composite samples captured the overall trend in concentration, but the dilution shortly after rain events was captured only barely or not at all, as opposed to the MS^{2}field samples in which the up to 50 % dilution was captured (Figure 3.3, SI-A).

The presence of chlorothalonil TPs in this catchment was already reported by Schorr et al. (2023). However, the TP R471811 could not be analyzed with the analytical method therein and is hence reported here with a median concentration of 250 ng/L and a maximum concentration of 410 ng/L in 42 h-composite samples (SI-B 2.2). Considering both studies, 4 TPs of chlorothalonil could be identified in the composite samples. Chlorothalonil TPs are still detected throughout Swiss

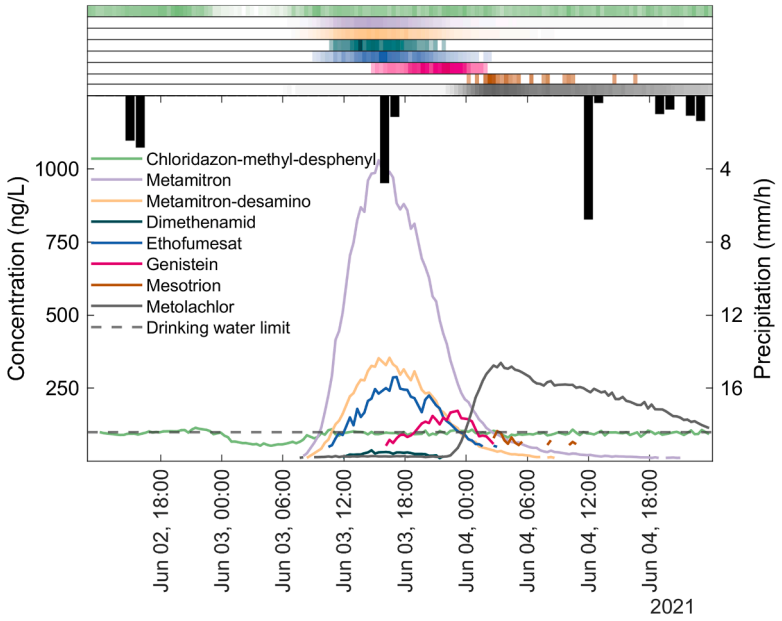

Fig. 3. Time series of different compounds detected during the 5th event in the beginning of June 2021. The heat maps on top refer to the various detected compounds.

groundwater samples in elevated concentrations (Hintze et al., 2021; Kiefer et al., 2019) despite the revoked approval of the active substance in 2019 (BLW, 2019), demonstrating the importance of monitoring TPs. Still, the potentially toxicologically relevant chlorothalonil TPs (EFSA, 2018) were found in groundwater only some 30 years later, in 2017 (Kiefer et al., 2019). A similar pattern could be identified for dimethachlor or terbuthylazine, for which only TPs were detected instead of their parent compounds (Table 1). Overall, the dilution of legacy compounds during rain events could only be observed in the MS^{2}field samples.

3.3.2. *Peak compounds – comparison with 42 h-composite samples*

Peak concentrations of pesticides following rain events have been observed before (e.g. Schiperski et al. (2015)), but here, the concentrations of several compounds were traced for the first time at a sufficiently high temporal resolution, showing their different breakthrough times and peak concentrations. Only two pesticides exceeding 100 ng/L would have been detected if only composite samples were considered. Generally, concentrations up to 4 times higher were found in the MS^{2}field samples compared to the 42 h-composite samples (Table 1). In event 5 (Table 2.6, SI-A), the highest number of compounds and the highest concentrations were detected. This included dimethenamid, ethofumesate, genistein, mesotrione, metamitron, metamitron-desamino, metolachlor, and tebuconazole (Table 1). Of those, four herbicides exceeded the Swiss drinking water limit of 100 ng/L for pesticides (Bundesrat, 1998) in this particular event. The maximum concentrations in the 5th event differed for each compound, ranging from ~40 to 1000 ng/L. Besides strongly varying peak concentrations between compounds per event, variations among events for the same compound were also observed. Metamitron and dimethenamid peak concentrations for example varied strongly between events within and after the MS^{2}field period (Figure 3.2, SI-A).

The dynamic of dimethenamid demonstrated the strong influence of the applied amount on pesticide detections. Dimethenamid was detected only after its main application in late June (after the MS^{2}field monitoring period) in considerable concentrations up to 790 ng/L in 42 h-composite samples during a rain-intensive period lasting from late June through mid-July (Figure 3.2, SI-A). Following the high concentration event in late June, dimethenamid continued to exceed 100 ng/L for

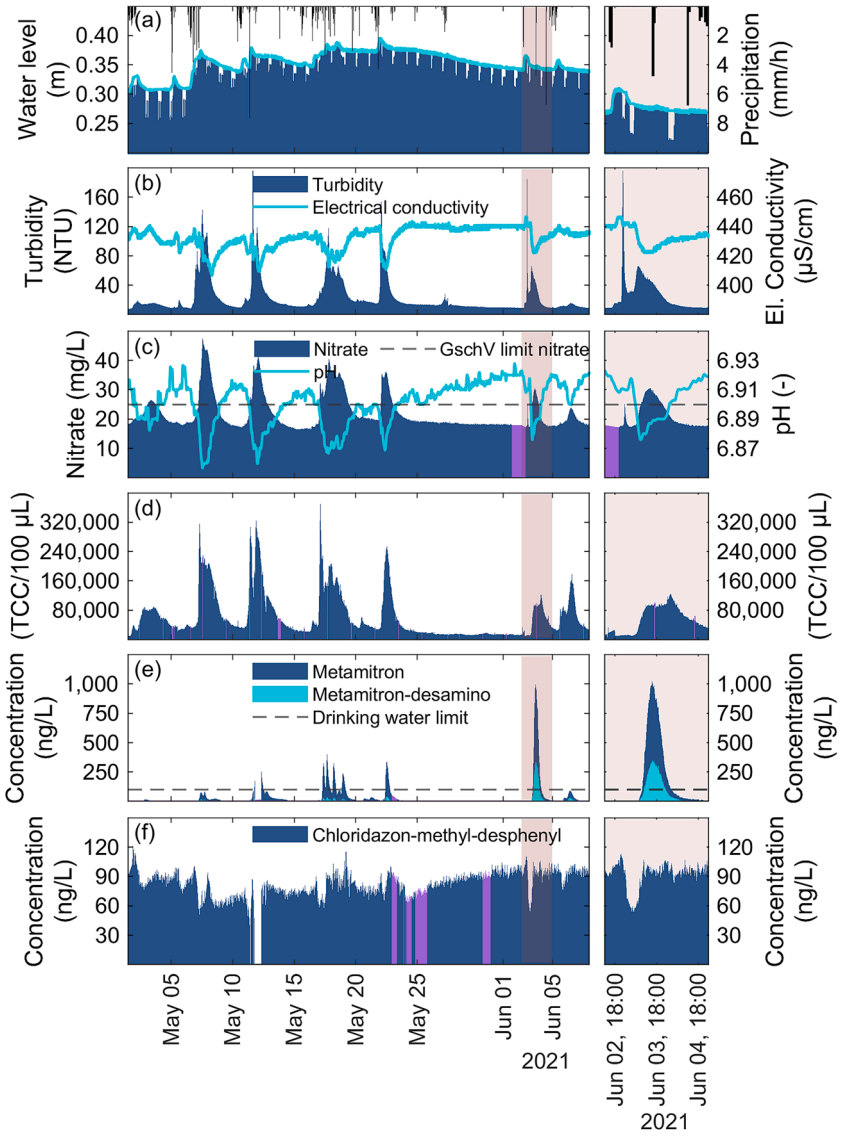

Fig. 4. Dynamics of contaminants and proxy parameters measured during the MS^{2}field monitoring period. This included: (a) water level & precipitation, (b) EC and turbidity, (c) nitrate and pH, (d) TCC, (e) metamitron with its TP, and (f) chloridazon-methyl-desphenyl. In the right graphs, the most pronounced event (marked brownish) is shown in higher resolution. Data jumps in water level were linearly interpolated (dark blue: original data, light blue: corrected data). Linearly interpolated data gaps in the time series of other parameters are visualized in purple. Values below the LOQ were replaced as described in subsection 2.6.

several days until the precipitation intensity decreased again. Also, its TPs were detected in elevated concentrations up to ca. 300 ng/L during that period (Schorr et al., 2023). Unfortunately however, this data set lacks flow path, soil moisture and spatially resolved precipitation information which does consequently not allow to relate precipitation intensity to detected concentrations.

The intra-event and inter-compound differences in peak height were apparent, most notably in event 5 (Fig. 3). First, chloridazon-methyl-desphenyl was diluted, and then metamitron (log P = 0.9), its TP metamitron-desamino, ethofumesate (log P = 2.7) and dimethenamid (log P = 1.9) broke through at roughly the same time. The next compound to break through was genistein, after which metolachlor (log P = 3.4) and mesotrione (log P = 0.1) broke through simultaneously (log P and GUS values from Lewis et al. (2016)). However, studying their log P or their GUS values did not yield a clear explanation for their varying breakthrough times, demonstrating that these descriptors can indicate whether a compound can break through at karst springs but not with which dynamics. According to the application data, metamitron and ethofumesat were applied on only one field close to the spring (~1–2 km), whereas dimethenamid and mesotrione were used throughout the catchment. Hence, the flow path might play a major role in break through times. According to the data, metolachlor was not applied and was thus attributed to a non-declared application. For genistein, a naturally occurring compound in soy beans and red clover (Fukutake et al., 1996; Saviranta et al., 2008), the origin remained unclear and consequently also the reasons for its distinct dynamic. To decipher the intra-event, inter-compound differences and the influence of compound physicochemical properties, specific tracer tests with different pesticides applied in only one location within the catchment would be needed in combination with a temporally resolved sampling. Regarding the exported load, a rough, back-on-the-envelope calculation with the average discharge at this spring yielded ~1 g of metamitron exported during event 5, equivalent to ca. 0.03 % of the mass applied (SI-B) between events 4 and 5 (full calculation in Section 4 in SI-A).

3.4. Correlation between proxies and spring contamination

The Spearman correlations between spring contaminants, including pesticides (and their TPs), nitrate and TCC, and the other monitored parameters termed as proxies, were studied. Focus was laid on metamitron and its TP since they were the only peak compounds that occurred during each of the six monitored events from late April to early June 2021 (Fig. 4). Also, they were the first ones to break through at the spring, and therefore most relevant from a water quality perspective. Further, the aim of this analysis was to study compounds that were mobilized by rain and subsequently broke through at the spring. Therefore, legacy compounds (e.g. chloridazon-methyl-desphenyl), which showed generally weak correlations with the proxies, were not further considered in this part of the analysis (details in Section 4 of SI-A). The time series of the contaminants as well as the proxies were visually inspected to delimit the events (SI-A). During the second event, MS^{2}field data was missing and was hence excluded from the correlation analysis.

During the whole MS^{2}field monitoring period, the contaminants showed co-occurring peaks after rain events with maximum pesticide concentrations (details in 3.3) and nitrate concentrations (45 mg/L) exceeding the national limit for drinking water (25 mg/L) as well as bacterial cell concentration peaks with up to ~300,000 cells/100 µL (Fig. 4). While nitrate and TCC phenomena have previously been observed in karst systems (Besmer et al., 2017; Huebsch et al., 2014; Opsahl et al., 2017), this is the first report of peak phenomena for pesticides and their TPs with such high temporal resolution. Proxy parameters on the other hand showed both, peak (water level, turbidity) and dilution phenomena (EC, pH). Here, the peaks in water level and turbidity were likely associated with piston flow and diffuse recharge combined (Ford and Williams, 2007) while the decrease in EC can be explained by the breakthrough of less mineralized meteoric water. The decrease in pH can be due to both, the lower pH of meteoric water (5.6–5.7, (Barrett and Brodin, 1955; Bogan et al., 2009)), and the mobilization of soil pore water rich in CO_2 (Pu et al., 2014). The changes in various monitored parameters occurred asynchronously, a behavior that was previously observed for other karst springs (Pronk et al., 2006;

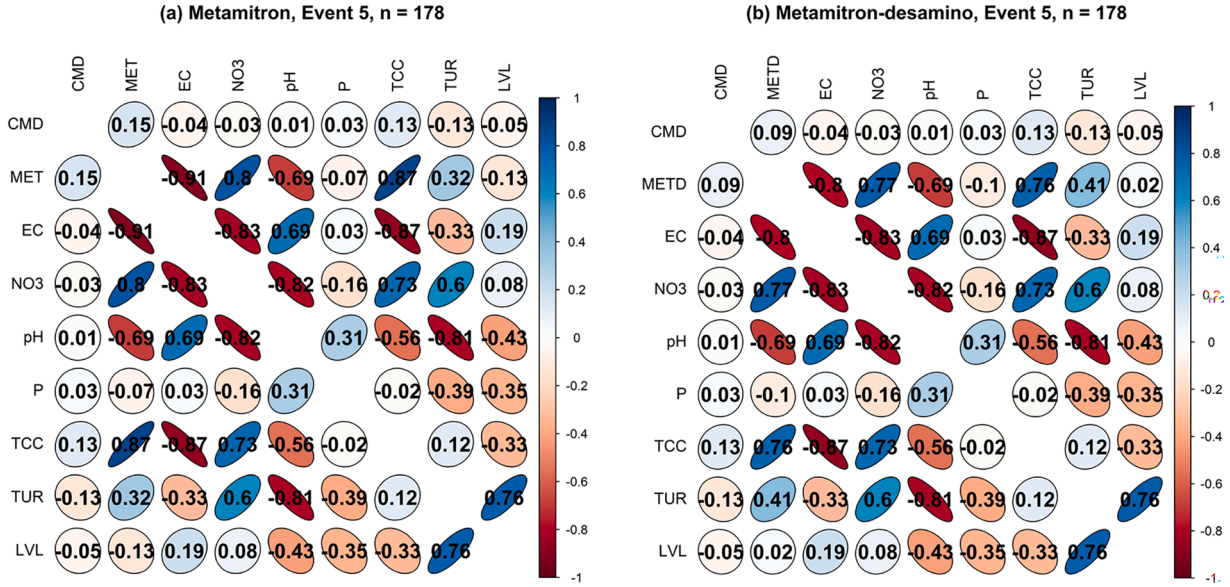

Fig. 5. Correlation analysis (spearman) of the re-sampled time series of event 5. To obtain data pairs at the same temporal resolution, all data were interpolated at 20 min time intervals (resolution of the MS^{2}field data). Samples in which (a) metamitron, and (b) metamitron-desamino concentrations were below LOQ, were replaced with ½ their respective LOQs. Abbreviations: CMD: chloridazon-methyl-desphenyl; MET: metamitron; METD: metamitron-desamino; EC: electrical conductivity; NO3: nitrate; P: precipitation; TCC: total cell count; TUR: turbidity; LVL: water level. EC, pH and water level time series were LOESS-smoothed (window = 50) before interpolation to remove noise and remove jumps present in the data due to rounding when the data was recorded. Correlations of other events are summarized in SI-C.

Schiperski et al., 2015) but is only observable with a high temporal resolution. The 5th rain event exhibited the highest pesticide concentrations (Fig. 3) and was preceded by a prolonged dry period, and is therefore shown in detail in the right column of Fig. 4.

To determine a suitable proxy parameter for spring contamination, the Spearman correlations between all the monitored parameters were calculated (Fig. 5). The contaminants were strongly correlating with each other indicating a similar origin and/or mobilization mechanism. The electrical conductivity and the pH correlate (very) strongly negatively with metamitron ($\rho_{EC\sim MET}$ = -0.91 & $\rho_{pH\sim MET}$ = -0.69, Fig. 5) and strongly negatively with its TP metamitron-desamino ($\rho_{EC\sim METD}$ = -0.8 & $\rho_{pH\sim METD}$ = -0.69, Fig. 5). Due to the strong association of the decrease in EC (Hillebrand et al., 2014) and in pH (Vesper and White, 2004) with the breakthrough of meteoric water, a mobilization of the contaminants with meteoric water is likely. Considering that metamitron was applied to a large part in the dry period before the 5th event (01.06.2021, SI-B 3), hence being present mainly at the catchment surface, this hypothesis becomes even more likely. The correlations between the contaminants, and EC and pH across all six events were in a similar range (Figure 4.1, SI-A), consolidating the findings of event 5. Therefore, especially at this site, but potentially also at others, EC and pH could be used as proxies for pesticide contamination, as was similarly found in (Hillebrand et al., 2014) for the relationship between metazachlor and EC.

Turbidity showed an overall strong correlation with nitrate ($\rho_{TUR\sim NO3}$ = 0.84, Figure 4.1, SI-A) but weaker correlations with metamitron, its TP and TCC (Figure 4.1, SI-A). It was shown in several studies that the interpretation of turbidity can be quite ambiguous (Epting et al., 2018; Pronk et al., 2007; Schiperski, 2018) which was confirmed here, as piston flow induced turbidity spikes preceding the main peak were detected, similar to the observation made by Jukić and Denić-Jukić (2023). This resulted in weak to moderate correlations between turbidity, and pesticides and TCC, respectively. As the water level is also strongly influenced by piston flow and concentrated recharge (shortcuts like sinkholes), its peak preceded the breakthrough of metamitron and its TP. This rendered the correlations between them weak ($\rho_{LVL\sim MET}$ = 0.32, $\rho_{LVL\sim METD}$ = 0.12, Figure 4.1, SI-A) and its use as a proxy disadvantageous. Precipitation showed the weakest correlations of all monitored proxy parameters. This was not surprising as there was already a time lag between rainfall and the earliest change in water levels, which was similarly observed for rivers (details in Section 4, SI-A). The robust prediction of pesticide breakthrough would necessitate an analysis capturing more events with multiple pesticides breaking through.

The correlations for all detected pesticides and events are given in SI-C but did not show as strong correlations with EC and pH as metamitron and its TP, due to less detections and later breakthrough times. For finding a fitting proxy for water quality monitoring, however, it is most important to determine when exactly the contaminants start to break through and hence, the breakthrough of metamitron, as one of the fastest leachable tracer, suffices for proxy identification.

3.5. Comparison of both study sites

A second site in the Swiss Jura was monitored for pesticides via 42 h-composite samples in 2021 and the MS^{2}field in 2022, and for physicochemical parameters to learn whether different springs behave similarly. At site 2 in 2021, peak and dilution phenomena similar to those observed at site 1 were observed for discharge, EC, nitrate, the spectral absorption coefficient (SAC) measured at 254 nm (SAC 254) and at 436 nm (SAC 436) (both enabling the estimation of the quantity of dissolved organic substances, Figure 5.1, SI-A), thus indicating that similar breakthrough curves of pesticides can be expected. Further, several substances were detected after rain events, even in the 42 h-composite samples, exceeding 100 ng/L (e.g. MCPA and tritosulfuron, data not shown). In 2022, an 8-week long MS^{2}field campaign was conducted, but the three observed rain events were insufficient to induce a breakthrough of a pesticide in the spring of more than 100 ng/L (c_{max} = 22 ng/L (metamitron), Figure 5.3, SI-A). Hence, despite similar application volumes and otherwise similar catchment characteristics as site 1, the lack of significant rain events led to a much lower number of detected substances at site 2 in 2022 than in 2021. Continuously detected compounds in 2022 included atrazine, atrazine-desethyl, chlorothalonil TP R817888, and bentazone (Figure 5.2, SI-A). These compounds were diluted during the small rain events observed, which, in combination with only sporadic detects of other pesticides and their TPs (all below 100 ng/L), confirms the decisive impact of precipitation amounts for spring contamination.

3.6. Implications for managing karst groundwater resources

This study confirms the necessity to manage karst aquifers differently from sedimentary aquifers, as proposed by Worthington and Ford (2011). The temporally highly resolved in-situ sampling and analysis with the MS^{2}field would only be feasible for some water suppliers. Instead, the response of more easy-to-measure parameters could be used as proxies in event-based monitoring for pesticides, as was proposed for bacteria (Besmer et al., 2017). The data from the two sites analyzed here suggests that changes in the often measured turbidity hold more ambiguity than those of EC or pH when used as proxies. Using these two parameters to predict the deterioration of karst raw water quality instead of monitoring organic chemicals and/or TCC directly is therefore preferable. However, transferability to other karst springs is not necessarily given, and therefore, correlations between the contaminants and physicochemical parameters like EC must first be determined individually for each spring.

4. Conclusions and outlook

Different factors have superimposed influences on detected peak concentrations of pesticides: (a) Availability of pesticides: The case of dimethenamid demonstrated that the fundamental influencing factors are the application point in time and the applied amount. Only after the extensive application in late June high concentrations of dimethenamid, exceeding the drinking water limit of 100 ng/L, were detected. (b) Compound physicochemical properties: As indicated previously, for compounds to be mobile, they need to be sufficiently polar, or better, anionic. Further, they must be stable enough to endure photolytic degradation at the surface during dry periods, and hydrolysis or microbial degradation during transport. (c) Precipitation: In this study, no particular influence of precipitation intensity, e.g. on peak height, could be observed. However, the lag phase between application and precipitation certainly influence the degree to which pesticides are degraded and how saturated the soils are. (d) Karst aquifer properties: Generally, the more the aquifer is karstified, the larger the conduits will be and, therefore, the more permeable the aquifer will be. Sinkholes and their location relative to the fields strongly influence the infiltration speed of meteoric water alongside the transport of mobilized contaminants through the soil or epikarst by channeling surface runoff rapidly towards the saturated zone. Despite the uncertainty exerted by many influencing factors, the following conclusions could be drawn:

- For the first time, high-temporal-resolution pesticide concentration, nitrate and TCC data have conclusively demonstrated an increased risk of karst spring contamination by multiple contaminants simultaneously following rainfall. The results presented here likely represent a worst case scenario for current climate conditions as the precipitation was significantly higher in the early summer 2021 than previous decades. However, the observations made here still provide evidence that such events in principle can occur.
- The temporally highly resolved MS^{2}field monitoring showed that the sampling frequency must be sufficiently high and adapted to the dynamics at each spring to detect the dynamics of contamination of

spring water. The detection of genistein, mesotrion and prochloraz in the MS^2field samples, but not in the 42 h-composite samples, indicates that labile, unexpected and less concentrated substances can only be captured with HRMS and in-situ methods.
- Prediction of a pesticide peak concentration is challenging due to the number of influencing factors. However, the correlation analysis indicates that EC and pH could be used as proxies for pesticides, nitrate, and bacterial contamination. This and a catchment land-use analysis should yield sufficient information if the respective spring is prone to short-term contamination, and thus if monitoring during rain events is advisable.

CRediT authorship contribution statement

Johannes Schorr: Writing – review & editing, Writing – original draft, Visualization, Validation, Methodology, Investigation, Formal analysis, Data curation, Conceptualization. **Franziska Jud:** Writing – review & editing, Methodology, Investigation, Data curation. **Daniele la Cecilia:** Writing – review & editing. **Birgit Beck:** Writing – review & editing, Methodology. **Philipp Longree:** Writing – review & editing, Methodology. **Heinz Singer:** Writing – review & editing, Methodology. **Juliane Hollender:** Writing – review & editing, Supervision, Resources, Project administration, Funding acquisition, Conceptualization.

Declaration of competing interest

Juliane Hollender reports financial support was provided by Federal Office for the Environment. If there are other authors, they declare that they have no known competing financial interests or personal relationships that could have appeared to influence the work reported in this paper.

Data availability

Data will be made available on request.

Funding

Funding for this work was kindly provided by the Swiss Federal Office for the Environment (FOEN).

Acknowledgements

This work was funded by the FOEN and we thank Stephanie Zimmermann from FOEN for her support and discussion. The authors thank the local farmers for providing the application data and the cantonal authorities for gathering that data. Further, we thank Jürg Sigrist and Frederik Hammes from the Eawag Environmental Microbiology department for their support in setting up the online flow cytometry system and assisting in the evaluation of the raw data. Also, we thank Andreas Scheidegger and Martin Frey for their consulting on statistical analysis.

The graphical abstract was partly created using Biorender (https://biorender.com).

Supplementary materials

Supplementary material associated with this article can be found, in the online version, at doi:10.1016/j.watres.2024.122412.

References

Bakalowicz, M., 2005. Karst groundwater: a challenge for new resources. Hydrogeol. J. 13, 148–160. https://doi.org/10.1007/s10040-004-0402-9.

Baran, N, Lepiller, M, Mouvet, C., 2008. Agricultural diffuse pollution in a chalk aquifer (Trois Fontaines, France): influence of pesticide properties and hydrodynamic constraints. J. Hydrol. 358, 56–69. https://doi.org/10.1016/j.jhydrol.2008.05.031.

Barrett, E, Brodin, G., 1955. The acidity of scandinavian precipitation. Tellus 7, 251–257. https://doi.org/10.1111/j.2153-3490.1955.tb01159.x.

Besmer, MD, Hammes, F, Sigrist, JA, Ort, C., 2017. Evaluating monitoring strategies to detect precipitation-induced microbial contamination events in karstic springs used for drinking water. Front. Microbiol. 8. https://doi.org/10.3389/fmicb.2017.02229.

Besmer, MD, Weissbrodt, DG, Kratochvil, BE, Sigrist, JA, Weyland, MS, Hammes, F., 2014. The feasibility of automated online flow cytometry for in-situ monitoring of microbial dynamics in aquatic ecosystems. Front. Microbiol. 5, 265. https://doi.org/10.3389/fmicb.2014.00265.

BLW. Approval for chlorothalonil is withdrawn with immediate effect (Zulassung für Chlorothalonil wird mit sofortiger Wirkung entzogen). (2019). Accessed: 22.11.2023. https://www.blw.admin.ch/blw/de/home/services/medienmitteilungen.msg-id-77491.html.

Bogan, RAJ, Ohde, S, Arakaki, T, Mori, I, McLeod, CW., 2009. Changes in rainwater pH associated with increasing atmospheric carbon dioxide after the industrial revolution. Water Air Soil Pollut. 196, 263–271. https://doi.org/10.1007/s11270-008-9774-0.

Bundesrat S. 814.201 Gewässerschutzverordnung (Water Protection Ordinance), 1998.

Butscher, C, Auckenthaler, A, Scheidler, S, Huggenberger, P., 2011. Validation of a numerical indicator of microbial contamination for karst springs. Groundwater 49, 66–76. https://doi.org/10.1111/j.1745-6584.2010.00687.x.

ChemAxon. JChem for Office was used for structure searching and log D calculation, JChem 23.5.0.480, 2023.

Coxon, C., 2011. Agriculture and Karst. In: Karst Management, pp. 103–138. https://doi.org/10.1007/978-94-007-1207-2_5.

Dormann, CF., 2013. Parametrische Statistik - Verteilungen, maximum likelihood und GLM in R. Springer Spektrum Berlin. https://doi.org/10.1007/978-3-642-34786-3.

Doummar, J, Geyer, T, Baierl, M, Nödler, K, Licha, T, Sauter, M., 2014. Carbamazepine breakthrough as indicator for specific vulnerability of karst springs: application on the Jeita spring, Lebanon. Appl. Geochem. 47, 150–156. https://doi.org/10.1016/j.apgeochem.2014.06.004.

EFSA, 2018. Peer review of the pesticide risk assessment of the active substance chlorothalonil. EFSA J. 16, 1–40. https://doi.org/10.2903/j.efsa.2018.5126.

Epting, J, Page, RM, Auckenthaler, A, Huggenberger, P., 2018. Process-based monitoring and modeling of Karst springs–Linking intrinsic to specific vulnerability. Sci. Total Environ. 625, 403–415. https://doi.org/10.1016/j.scitotenv.2017.12.272.

FOEN. Zustand und Entwicklung Grundwasser Schweiz, Ergebnisse der Nationalen Grundwasserbeobachtung NAQUA, Stand 2016. Bundesamt für Umwelt, Bern. Umwelt-Zustand Nr. 1901: 138 S. (2019).

FOEN. Nationale Grundwasserbeoachtung NAQUA. (2020). Accessed: 21.11.2023. https://www.bafu.admin.ch/bafu/de/home/themen/wasser/fachinformationen/zustand-der-gewaesser/zustand-des-grundwassers/grundwasser-qualitaet/pestizide-im-grundwasser.html.

FOEN. (2023). Accessed: 01.09.2023. https://www.bafu.admin.ch/bafu/de/home.html.

Ford, D, Williams, PD, 2007. Karst Hydrogeology and Geomorphology. John Wiley & Sons.

Fukutake, M, Takahashi, M, Ishida, K, Kawamura, H, Sugimura, T, Wakabayashi, K., 1996. Quantification of genistein and genistin in soybeans and soybean products. Food Chem. Toxicol. 34, 457–461. https://doi.org/10.1016/0278-6915(96)87355-8.

Goldscheider, N, Chen, Z, Auler, AS, Bakalowicz, M, Broda, S, Drew, D, Hartmann, J, Jiang, G, Moosdorf, N, Stevanovic, Z, Veni, G., 2020. Global distribution of carbonate rocks and karst water resources. Hydrogeol. J. 28, 1661–1677. https://doi.org/10.1007/s10040-020-02139-5.

Gruber, K, Courteau, B, Bokhoree, M, McMahon, E, Kotz, J, Nienow, A., 2021. Photolysis of the herbicide dicamba in aqueous solutions and on corn (Zea mays) epicuticular waxes. Environ. Sci. Processes Impacts 23, 786–802. https://doi.org/10.1039/D1EM00058F.

Gustafson, DI., 1989. Groundwater ubiquity score: a simple method for assessing pesticide leachability. Environ. Toxicol. Chem. 8, 339–357. https://doi.org/10.1002/etc.5620080411.

Hillebrand, O, Nödler, K, Geyer, T, Licha, T., 2014. Investigating the dynamics of two herbicides at a karst spring in Germany: Consequences for sustainable raw water management. Sci. Total Environ. 482, 193–200. https://doi.org/10.1016/j.scitotenv.2014.02.117.

Hillebrand, O, Nödler, K, Licha, T, Sauter, M, Geyer, T., 2012. Identification of the attenuation potential of a karst aquifer by an artificial dualtracer experiment with caffeine. Water Res. 46, 5381–5388. https://doi.org/10.1016/j.watres.2012.07.032.

Hintze, S, Hannalla, YSB, Guinchard, S, Hunkeler, D, Glauser, G., 2021. Determination of chlorothalonil metabolites in soil and water samples. J. Chromatogr. A 1655, 462507. https://doi.org/10.1016/j.chroma.2021.462507.

Huebsch, M, Fenton, O, Horan, B, Hennessy, D, Richards, KG, Jordan, P, Goldscheider, N, Butscher, C, Blum, P., 2014. Mobilisation or dilution? Nitrate response of karst springs to high rainfall events. HESS 18, 4423–4435. https://doi.org/10.5194/hess-18-4423-2014.

Jukić, D, Denić-Jukić, V., 2023. An alternative approach to investigation of sediment transport through a karst aquifer. J. Hydrol. 625, 130037. https://doi.org/10.1016/j.jhydrol.2023.130037.

Kaiser, RA, Polk, JS, Datta, T, Parekh, RR, Agga, GE., 2022. Occurrence of antibiotic resistant bacteria in urban karst groundwater systems. Water 14. https://doi.org/10.3390/w14060960.

Kiefer, K, Bader, T, Minas, N, Salhi, E, Janssen, EM-L, von Gunten, U, Hollender, J., 2020. Chlorothalonil transformation products in drinking water resources: Widespread and

challenging to abate. Water Res. 183, 116066. https://doi.org/10.1016/j.watres.2020.116066.
Kiefer, K, Müller, A, Singer, H, Hollender, J., 2019. New relevant pesticide transformation products in groundwater detected using target and suspect screening for agricultural and urban micropollutants with LC-HRMS. Water Res. 165, 114972. https://doi.org/10.1016/j.watres.2019.114972.
Kolpin, DW, Schnoebelen, DJ, Thurman, EM., 2004. Degradates provide insight to spatial and temporal trends of herbicides in ground water. Groundwater 42, 601–608. https://doi.org/10.1111/j.1745-6584.2004.tb02628.x.
la Cecilia, D, Dax, A, Ehmann, H, Koster, M, Singer, H, Stamm, C., 2021. Continuous high-frequency pesticide monitoring to observe the unexpected and the overlooked. Water Res. X 13, 100125. https://doi.org/10.1016/j.wroa.2021.100125.
la Cecilia, D, Maggi, F, 2017. In-situ atrazine biodegradation dynamics in wheat (Triticum) crops under variable hydrologic regime. J. Contam. Hydrol. 203, 104–121. https://doi.org/10.1016/j.jconhyd.2017.05.004.
Lewis, KA, Tzilivakis, J, Warner, DJ, Green, A., 2016. An international database for pesticide risk assessments and management. Hum. Ecol. Risk Assess. Int. J. 22, 1050–1064. https://doi.org/10.1080/10807039.2015.1133242.
Maggi, F, Tang, FHM, la Cecilia, D, McBratney, A., 2019. PEST-CHEMGRIDS, global gridded maps of the top 20 crop-specific pesticide application rates from 2015 to 2025. Sci. Data 6, 170. https://doi.org/10.1038/s41597-019-0169-4.
Medici, G, West, LJ., 2021. Groundwater flow velocities in karst aquifers; importance of spatial observation scale and hydraulic testing for contaminant transport prediction. Environ. Sci. Pollut. Res. 28, 43050–43063. https://doi.org/10.1007/s11356-021-14840-3.
Metcalfe, CD, Beddows, PA, Bouchot, GG, Metcalfe, TL, Li, H, Van Lavieren, H., 2011. Contaminants in the coastal karst aquifer system along the Caribbean coast of the Yucatan Peninsula, Mexico. Environ. Pollut. 159, 991–997. https://doi.org/10.1016/j.envpol.2010.11.031.
Morasch, B., 2013. Occurrence and dynamics of micropollutants in a karst aquifer. Environ. Pollut. 173, 133–137. https://doi.org/10.1016/j.envpol.2012.10.014.
NABODAT. NABODAT: das nationale Bodeninformationssystem. (2024). Accessed: 12.03.2024. https://www.nabodat.ch/.
Opsahl, SP, Musgrove, M, Slattery, RN., 2017. New insights into nitrate dynamics in a karst groundwater system gained from in situ high-frequency optical sensor measurements. J. Hydrol. 546, 179–188. https://doi.org/10.1016/j.jhydrol.2016.12.038.
Padilla, IY, Vesper, DJ, 2018. Fate, transport, and exposure of emerging and legacy contaminants in karst systems: state of knowledge and uncertainty. Karst groundwater contamination and public health. Adv. Karst Sci. 33–49. https://doi.org/10.1007/978-3-319-51070-5_5.
Parise, M, Gabrovsek, F, Kaufmann, G, Ravbar, N., 2018. Advances in Karst Research: Theory, Fieldwork and Applications, 466. Geological Society, London, Special Publications, pp. 217–236. https://doi.org/10.1144/sp466.26.
Prest, EI, Hammes, F, Kötzsch, S, van Loosdrecht, MCM, Vrouwenvelder, JS., 2013. Monitoring microbiological changes in drinking water systems using a fast and reproducible flow cytometric method. Water Res. 47, 7131–7142. https://doi.org/10.1016/j.watres.2013.07.051.
Pronk, M, Goldscheider, N, Zopfi, J., 2006. Dynamics and interaction of organic carbon, turbidity and bacteria in a karst aquifer system. Hydrogeol. J. 14, 473–484. https://doi.org/10.1007/s10040-005-0454-5.
Pronk, M, Goldscheider, N, Zopfi, J., 2007. Particle-size distribution as indicator for fecal bacteria contamination of drinking water from karst springs. Environ. Sci. Technol. 41, 8400–8405. https://doi.org/10.1021/es071976f.
Pu, J, Yuan, D, Zhao, H, Shen, L., 2014. Hydrochemical and PCO2 variations of a cave stream in a subtropical karst area, Chongqing, SW China: piston effects, dilution effects, soil CO2 and buffer effects. Environ. Earth Sci. 71, 4039–4049. https://doi.org/10.1007/s12665-013-2787-z.
Ravbar, N, Goldscheider, N., 2007. Proposed methodology of vulnerability and contamination risk mapping for the protection of karst aquifers in Slovenia. Acta Carsol. 36. https://doi.org/10.3986/ac.v36i3.174.
Reberski, JL, Terzić, J, Maurice, LD, Lapworth, DJ., 2022. Emerging organic contaminants in karst groundwater: a global level assessment. J. Hydrol. 604, 127242. https://doi.org/10.1016/j.jhydrol.2021.127242.
Reh, R, Hillebrand, O, Geyer, T, Nödler, K, Licha, T, Sauter, M., 2014. Charakterisierung zweier Karstsysteme mithilfe organischer Spurenstoffe. Grundwasser 19, 251–262. https://doi.org/10.1007/s00767-014-0264-6.
Reh, R, Licha, T, Geyer, T, Nödler, K, Sauter, M., 2013. Occurrence and spatial distribution of organic micro-pollutants in a complex hydrogeological karst system during low flow and high flow periods, results of a two-year study. Sci. Total Environ. 443, 438–445. https://doi.org/10.1016/j.scitotenv.2012.11.005.
Reh, R, Nödler, K, Hillebrand, O, Licha, T., 2016. Potenziale der Nutzung organischer Spurenstoffe als Indikatoren in Grundwasserleitern. Grundwasser 21, 289–293. https://doi.org/10.1007/s00767-016-0338-8.
SANTE/12682/2019. Main changes introduced in Document N° SANTE/12682/2019 with respect to the previous version (Document N° SANTE/11813/2017). Guidance document on analytical quality control and method validation procedures for pesticide residues analysis in food and feed (2019).
Saviranta, NMM, Anttonen, MJ, von Wright, A, Karjalainen, RO, 2008. Red clover (Trifolium pratense L.) isoflavones: determination of concentrations by plant stage, flower colour, plant part and cultivar. J. Sci. Food Agric. 88, 125–132. https://doi.org/10.1002/jsfa.3056.
Schaffer, M, Licha, T., 2015. A framework for assessing the retardation of organic molecules in groundwater: Implications of the species distribution for the sorption-influenced transport. Sci. Total Environ. 524, 187–194. https://doi.org/10.1016/j.scitotenv.2015.04.006.
Schiperski, F., 2018. Turbidity as an indicator of contamination in karst springs: a short review. In: Karst Groundwater Contamination and Public Health, pp. 127–139. https://doi.org/10.1007/978-3-319-51070-5_14.
Schiperski, F, Zirlewagen, J, Hillebrand, O, Nödler, K, Licha, T, Scheytt, T., 2015. Relationship between organic micropollutants and hydro-sedimentary processes at a karst spring in south-west Germany. Sci. Total Environ. 532, 360–367. https://doi.org/10.1016/j.scitotenv.2015.06.007.
Schorr, J, Therampilly, S, Jiao, L, Longree, P, Singer, H, Hollender, J., 2023. Closing the gap: Ion chromatography coupled to high-resolution mass spectrometry to trace highly polar anionic substances in groundwater. Sci. Total Environ., 164170 https://doi.org/10.1016/j.scitotenv.2023.164170.
Selak, A, Reberski, JL, Klobučar, G., 2023. Assessing the persistence, mobility and toxicity of emerging organic contaminants in Croatian karst springs used for drinking water supply. Sci. Total Environ. 903, 166240. https://doi.org/10.1016/j.scitotenv.2023.166240.
Stravs, MA, Stamm, C, Ort, C, Singer, H., 2021. Transportable automated HRMS platform "MS2field" enables insights into water-quality dynamics in real time. Environ. Sci. Technol. Lett. 8, 373–380. https://doi.org/10.1021/acs.estlett.1c00066.
Stroj, A, Briški, M, Oštrić, M., 2020. Study of groundwater flow properties in a karst system by coupled analysis of diverse environmental tracers and discharge dynamics. Water 12. https://doi.org/10.3390/w12092442.
Tian, Z, Zhao, H, Peter, KT, Gonzalez, M, Wetzel, J, Wu, C, Hu, X, Prat, J, Mudrock, E, Hettinger, R, Cortina, AE, Biswas, RG, Kock, FVC, Soong, R, Jenne, A, Du, B, Hou, F, He, H, Lundeen, R, Gilbreath, A, Sutton, R, Scholz, NL, Davis, JW, Dodd, MC, Simpson, A, McIntyre, JK, Kolodziej, EP., 2021. A ubiquitous tire rubber–derived chemical induces acute mortality in coho salmon. Science 371, 185–189. https://doi.org/10.1126/science.abd6951.
Vesper, DJ, Loop, CM, White, WB., 2001. Contaminant transport in karst aquifers. Theor. Appl. Karstol. 13, 101–111.
Vesper, DJ, White, WB., 2004. Storm pulse chemographs of saturation index and carbon dioxide pressure: implications for shifting recharge sources during storm events in the karst aquifer at Fort Campbell, Kentucky/Tennessee, USA. Hydrogeol. J. 12, 135–143. https://doi.org/10.1007/s10040-003-0299-8.
Worthington, SRH, Ford, DC., 2011. Self-organized permeability in carbonate aquifers. Groundwater 47, 326–336. https://doi.org/10.1111/j.1745-6584.2009.00551.x.
Zemann, M, Wolf, L, Grimmeisen, F, Tiehm, A, Klinger, J, Hötzl, H, Goldscheider, N., 2015. Tracking changing X-ray contrast media application to an urban-influenced karst aquifer in the Wadi Shueib, Jordan. Environ. Pollut. 198, 133–143. https://doi.org/10.1016/j.envpol.2014.11.033.
Zirlewagen, J, Licha, T, Schiperski, F, Nödler, K, Scheytt, T., 2016. Use of two artificial sweeteners, cyclamate and acesulfame, to identify and quantify wastewater contributions in a karst spring. Sci. Total Environ. 547, 356–365. https://doi.org/10.1016/j.scitotenv.2015.12.112.